

Power Augmentation of a Horizontal Axis Wind Turbine Using a Mie Type Tip Vane: Velocity Distribution Around the Tip of a HAWT Blade With and Without a Mie Type Tip Vane

Y. Shimizu

H. Imamura

S. Matsumura

T. Maeda

Department of Mechanical Engineering,
Mie University,
1515 Kamihama-cho, Tsu, Mie 514, Japan

G. J. W. van Bussel

Institute for Wind Energy,
Delft University of Technology,
Stevinweg 1, The Netherlands

Power augmentation and velocity measurements in the wake of a HAWT blade with Mie type tip vane (a tip device on the main blade) are presented. The maximum C_p with a Mie type tip vane is found to be 15 percent larger than that without the Mie type tip vane. Power augmentation caused by the Mie type tip vane is mainly due to the reduction of tip vortex and the diffusing effect by the Mie type tip vane. The effects of a Mie type tip vane are quantitatively verified by the velocity distributions around the tip of the main blade. The velocity distribution was measured by three-dimensional hot wire probes, which measured the axial, radial, and tangential velocity components. The circulation distributions along the main blade with a Mie type tip vane and without a Mie type tip vane were obtained from the measured velocity distributions. A strong reduction of bound vorticity is found for the main blade tip without the Mie type tip vane, whereas the bound vorticity persists on the main blade tip with the Mie type tip vane.

Introduction

The idea of the power augmentation of a horizontal axis wind turbine by installing a tip vane on the blade tip was proposed by Van Bussel (1986), Van Holten (1976), and G. W. Gyatt and P. B. S. Lissaman, Aero Vironment Inc. (1985). The effectiveness of a Delft type tip vane, which was proposed by Van Holten and Van Bussel, has been proven theoretically. The Aero Vironment Inc. type tip vane was practically applied to a horizontal axis wind turbine and succeeded to improve the output of the wind turbine. Shimizu et al. (1990, 1991, 1994a, 1994b) proposed another type tip vane, namely, the Mie type tip vane, and demonstrated that the power of a wind turbine increases remarkably as a result of attaching the Mie type tip vane to the tip of the main blade. The effects of the Mie type tip vane have been mainly determined as follows:

- (1) The induced velocity in the rotor plane decreases due to the displacement of the tip vortex.
- (2) The input energy available for the wind turbine rises because the area of the captured stream tube increases due to a diffuser effect.
- (3) The rotational speed of the rotor can be controlled by changing the installation angle of the Mie type tip vane (Shimizu et al., 1994c).

The effects (1) and (2) were qualitatively confirmed by flow visualization techniques, including the tuft grid method and the smoke flow method with vapor paraffin (Shimizu et al., 1994b). More quantitative measurements still remain to be carried out further. This paper shows the axial, radial, and tangential components of the velocity measured in the wake near the rotor

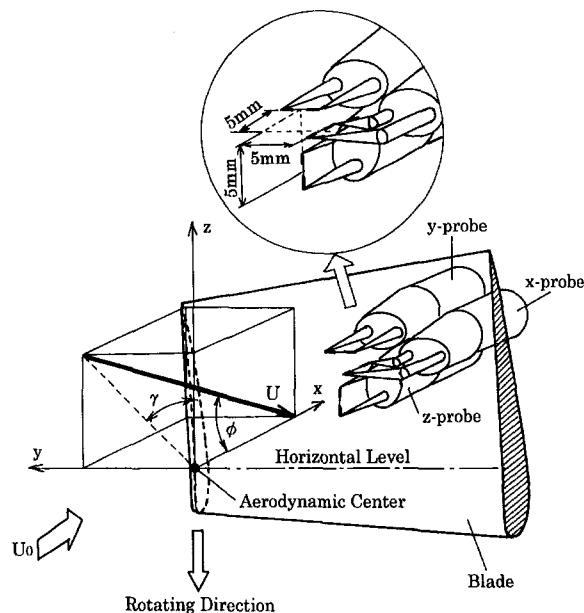


Fig. 1 Coordinate system in experiments and shape of probes

plane and near the blade tip. The measurements are carried out using the three-dimensional hot wire probes, which have good performance for the signal response to the velocity fluctuation. The results of this experiment demonstrate the above effects (1) and (2) due to the Mie type tip vane.

Experimental Apparatus and Procedure

Wind Tunnel and Wind Turbine. Figure 1 shows the coordinate system used in this study. It is referred to the main

Contributed by the Solar Energy Division of THE AMERICAN SOCIETY OF MECHANICAL ENGINEERS for publication in the ASME JOURNAL OF SOLAR ENERGY ENGINEERING. Manuscript received by the ASME Solar Energy Division, Jan. 1995; final revision, May 1995. Associate Technical Editor: P. S. Veers.

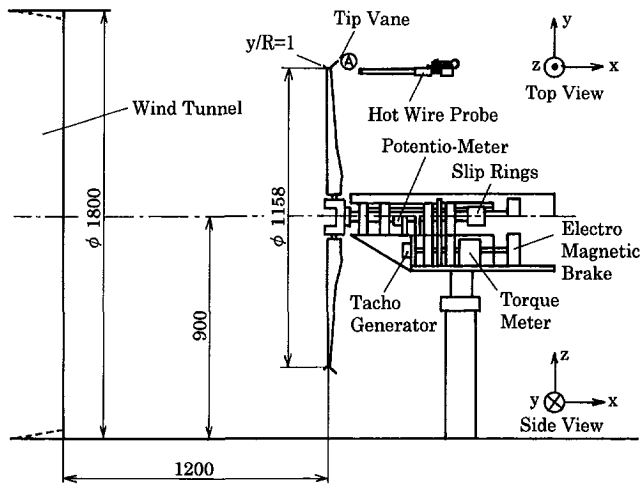


Fig. 2 Experimental apparatus

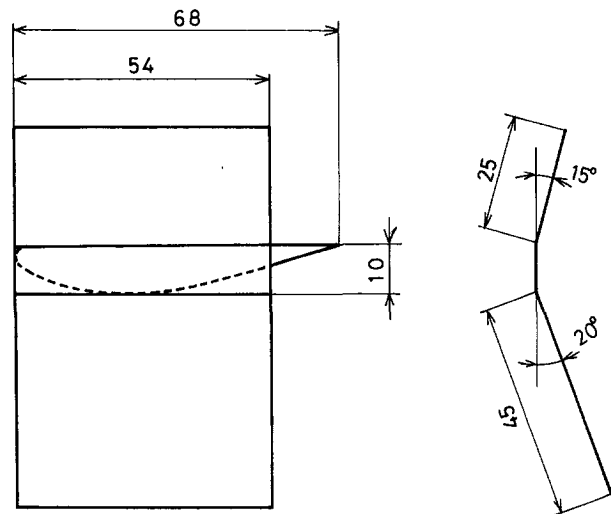


Fig. 3 Configuration of a V-type Mie type tip vane on a blade tip

blade of the rotor, set in the horizontal position. This coordinate system is fixed in the horizontal plane.

Figure 2 shows the experimental equipment. The wind tunnel has a outlet diameter of 1.8 m, and it is an open jet type. The wind speed in the tunnel reaches a maximum value of 15 m/s and its turbulence intensity remains below 1.8 percent. The turbulence intensity to the tip speed of blade is kept below 0.9 percent at the optimum tip-speed ratio. The test wind turbine has a diameter of 1.158 m. It has two blades which are twisted and tapered, and equipped with FX74-CL6-140 airfoil-sections. The twist angle is given in the previous papers (Shimizu et al., 1994a and 1994b). The main blade has a tip radius of 0.579 m, a spanwise length of 0.500 m and a aspect ratio of 5.970.

The wind turbine is located at 1.2 m, downwind of the outlet of wind tunnel. In order to minimize the influence of jet disturbance on the flow at the model rotor, a free space of 4.6 m is taken downwind of the turbine.

In this paper we use the V-type Mie vane (Fig. 3) because of its higher efficiency as shown in previous studies (Shimizu et al., 1991, 1994a, 1994b). The Mie vane has a chord length of 54 mm, and it is 80 percent length relative to the tip chord of main blade, 68 mm. The Mie vane is made of aluminum plate of 1 mm thickness.

Figure 4 shows the relation between the power coefficient C_p and the tip speed ratio λ . It has been shown that, in the case of the turbine with the Mie vane, the power at the optimum efficiency point is improved by 15 percent compared with the value without the Mie vane (Shimizu et al., 1991).

Hot Wire Probes. In order to measure the axial, radial, and tangential components of the wind velocity, three-dimensional hot wire probes are used as shown in Fig. 1. The distance of the prongs of each probe is held at 3 mm. Tungsten filaments of diameter 5 μ m, which both end parts plated with copper exclusive of the middle part of 1 mm, are used as hot wires.

Nomenclature

R = radius of wind turbine blade (m)
 U = resultant velocity of u , v , and w (m/s)
 U_0 = wind velocity upwind the wind turbine (m/s)
 u , v , w = velocity components of the x , y , and z direction, respectively (m/s)

Δu , Δw = amplitude of u and w due to blade passage, respectively (m/s)
 x , y , z = axial, radial, and tangential coordinate, respectively (m)
 Γ = circulation strength around the blade (m^2/s)

λ = tip-speed ratio, $R\omega/U_0$
 Ψ = azimuth angle (deg)
 ω = angular velocity of rotor revolution (rad/s)

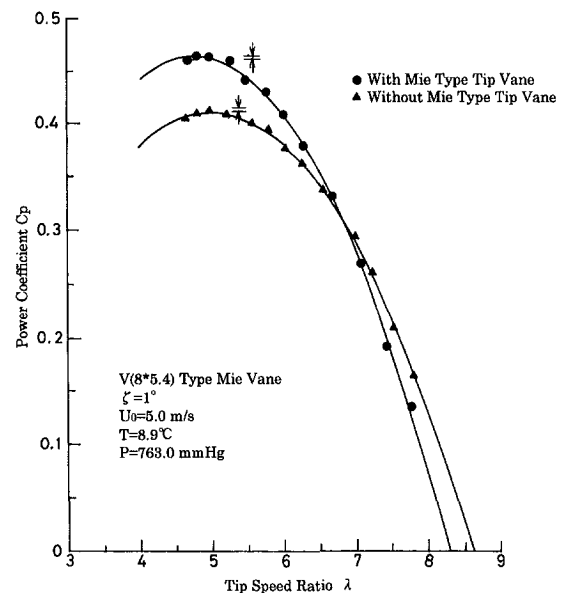


Fig. 4 Power coefficient of a model wind turbine rotor with and without a Mie type tip vane (uncertainty in $C_p = 0.4 \pm 0.002$ and $\lambda = 5 \pm 0.02$)

Experimental Technique. The wind velocity downwind of the turbine is measured using three hot wire probes. The experiments are carried out with a fixed wind velocity $U_0 = 5$ m/s and a tip-speed ratio $\lambda = 5$, which is shown to be the optimum efficiency of the test turbine. In this condition a Reynolds number of 1.3×10^5 is obtained, referring to the chord length and the rotational speed at the blade tip. The results of

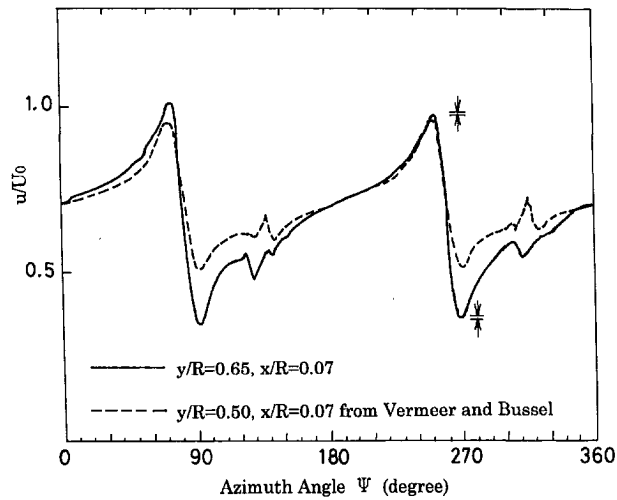


Fig. 5 Velocity variation due to blade passage without a tip vane (uncertainty in $u/U_0 = 1.0 \pm 0.005$ and $\Psi = 360 \pm 1$)

the measurements with the Mie type tip vane are compared with those without vane.

The azimuthal position of the blade is detected by a potentiometer.

All the output of three hot wire anemometers and the potentiometer are sampled by a PC with an A/D-converter. The sam-

pling frequency is 2.8 kHz, which corresponds to 3 deg for the azimuth angle of the blade.

The output from the anemometers is sampled over ten rotor revolutions. The sampled data are processed by the computer to the ensemble-averaged ones per one revolution.

Figure 5 shows an example of the axial wind velocity against the azimuth angle. The results of this experiment is shown by the solid lines in the figure. The dashed lines show the results from Vermeer and Bussel (1989). The blades pass the probes at azimuth angles 90 and 270 deg. It is seen that the wind velocity changes periodically because the blades pass the measuring point with the rotor rotation every 180 deg.

Results and Discussion

Ensemble-Averaged Velocity. The changes of all the three components of the ensemble-averaged velocities for the rotor without the Mie type tip vanes, at an axial position $x/R = 0.05$ and 0.12, are shown in Figs. 6(a) and 6(b), respectively. The dotted, the solid, and the chain line indicate the values at the $y/R = 1.00, 0.91,$ and $0.74,$ respectively. Three main features are highlighted as follows:

(1) The velocity components at arbitrary radial positions, $y/R < 1,$ rapidly change at the moment when the blades pass the probes. The axial component u increases with the blade approaching the probes, and rapidly drops just after the blade passage. After that, the component u increases again. The tangential component w rapidly increases at the moment of the

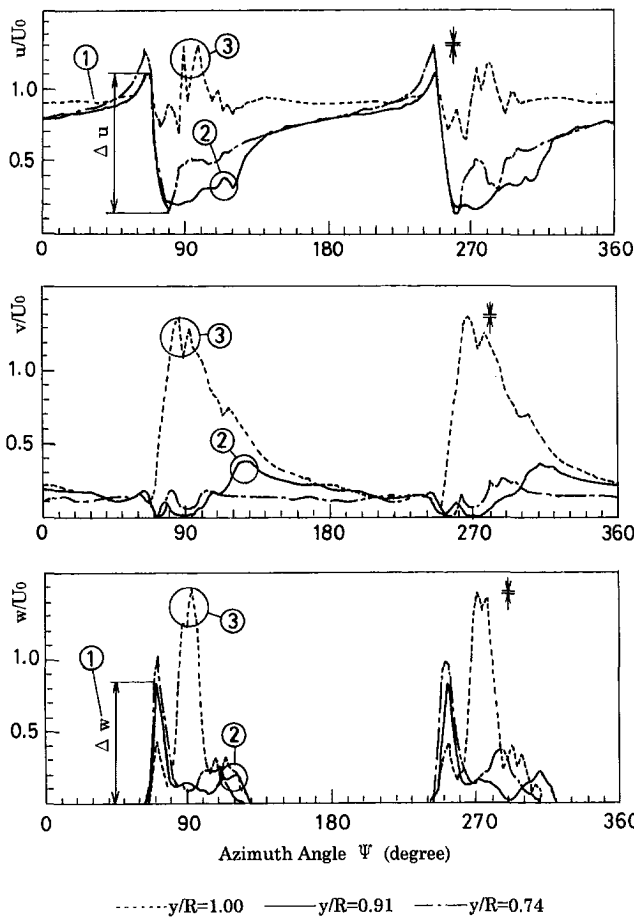


Fig. 6(a) Three components (axial, tangential, radial) of velocity distributions downwind of the model wind turbine rotor without a Mie type tip vane ($x/R = 0.05$); (uncertainty in $u/U_0 = 1.3 \pm 0.006,$ $v/U_0 = 1.4 \pm 0.006,$ $w/U_0 = 1.4 \pm 0.006$ and $\Psi = 360 \pm 1$)

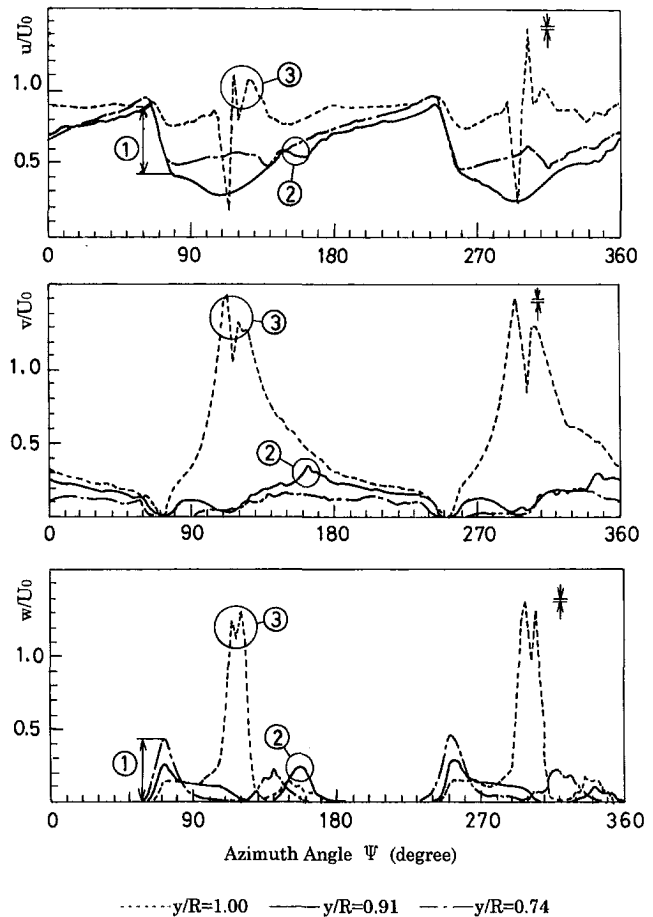


Fig. 6(b) Three components (axial, tangential, radial) of velocity distributions downwind of the model wind turbine rotor without a Mie type tip vane ($x/R = 0.12$); (uncertainty in $u/U_0 = 1.3 \pm 0.006,$ $v/U_0 = 1.4 \pm 0.006,$ $w/U_0 = 1.4 \pm 0.006$ and $\Psi = 360 \pm 1$)

blade passage. The azimuth angle for the rapid changes of the velocities (marked by ①) is independent of the downwind position of the probes. The magnitude of the velocity fluctuations, Δu and Δw , decrease with increasing the distance from the rotor plane and with increasing the radial distance towards the blade tip. The velocity changes (①) are caused by the velocity induced by the bound vorticity on the blade (Tutui, 1988; Vermeer and Bussel, 1989). The effects of the bound vorticity at the blade are always seen in the same azimuthal position.

(2) After the velocity fluctuations due to the bound vorticity (①) are observed, all the velocity components, u , v , and w are disturbed within a certain range of the azimuth angles, (marked by ②). The azimuth angle for these velocity fluctuations (②) depend on the axial distance of the probes from the rotor plane. The disturbance (②) appears at a later azimuth angle when the distance of the probes from the rotational plane is increased. The disturbance (②) is caused by the vortex sheet released from the trailing edge of the blade. The vortex sheet itself is enclosed in the turbulent boundary layer emanated from the rotor plane, so that the disturbance is observed for all the velocity components.

(3) In the area of the blade tip, $y/R = 1.00$, the increase in the velocity (marked by ③) is seen for all the velocity components, u , v , and w , after the fluctuation due to the bound vorticity, (①).

The velocity fluctuation (③) is not seen inside the rotor plane, ($y/R < 1.00$), and it is limited within the area near the blade tip. The position of the fluctuation (③) is observed later downstream the axial position, Fig. 6(b), which is similar to the characteristic (2). We can thus postulate that the velocity fluctuation (③) is caused by the tip vortex. Note that the velocity fluctuation due to the bound vorticity, (①), takes a small value at the blade tip.

Figure 7 shows three velocity components of the wake downwind of the blade with Mie vane. The measurements are carried out at the same positions as shown in Fig. 6. The local disturbance (②) caused by the tip vortex, which was observed in Fig. 6, is absent and the fluctuation (①) due to the blade passage is remarkably persistent. In particular, the velocity fluctuation (③) due to the tip vortex is seldom observed in the region of $0 < x/R < 0.073$ which corresponds to the downwind extension of the Mie vane. These phenomena are explained by the bound vorticity at the blade, which is transferred to the downwind side of the Mie vane. A theoretical survey of this effect is given by Van Bussel (1990).

Figure 8 shows the velocity components downwind of the Mie vane. The solid line represents the velocity fluctuation just inside the Mie vane $x/R = 0.09$ and $y/R = 1.02$, and the dashed line shows just outside the Mie vane $x/R = 0.09$ and $y/R = 1.03$. It is seen that the velocity changes rapidly due to the vortex, (marked by ④), which is similar to the fluctuation (③) in Fig. 6. From this examination, it is confirmed that the position at which the bound vortex is released, shifts toward the downstream edge of the Mie vane.

In the case of the velocity measurements with a Mie vane, the two main features (1) and (2) mentioned in the discussion above can be recognized.

Velocity Fluctuation at Blade Passage. Figures 9 and 10 show the spanwise variation of the velocity fluctuation amplitude due to blade passage, Δu and Δw , respectively, as denoted by ① in Figs. 6(a) and 6(b).

For the blade without a Mie vane, Δu the amplitude of the axial velocity variations decreases in the radial region of $0.9 < y/R < 1.0$ as shown in Fig. 9. On the contrary, the amplitude Δu for the blade with the Mie vane increases in the region of $0 < x/R < 0.073$ and $y/R < 1.0$. Moreover, such tendency is remarkable near the blade tip. In the downwind region of the Mie vane, $0.073 < x/R$, the amplitude Δu decreases more

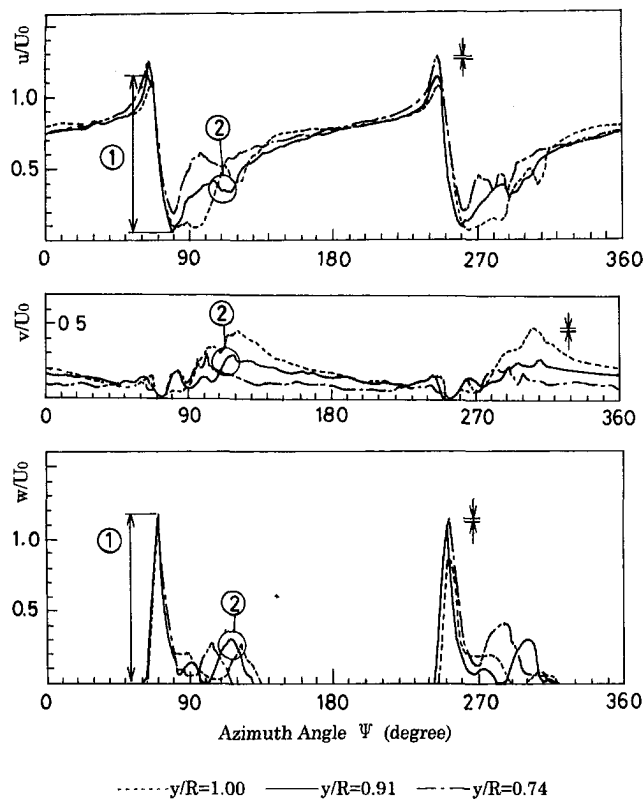


Fig. 7(a) Three components (axial, tangential, radial) of velocity distributions downwind of the model wind turbine rotor with a Mie type tip vane ($x/R = 0.05$); (uncertainty in $u/U_0 = 1.3 \pm 0.006$, $v/U_0 = 0.5 \pm 0.002$, $w/U_0 = 1.1 \pm 0.005$ and $\Psi = 360 \pm 1$)

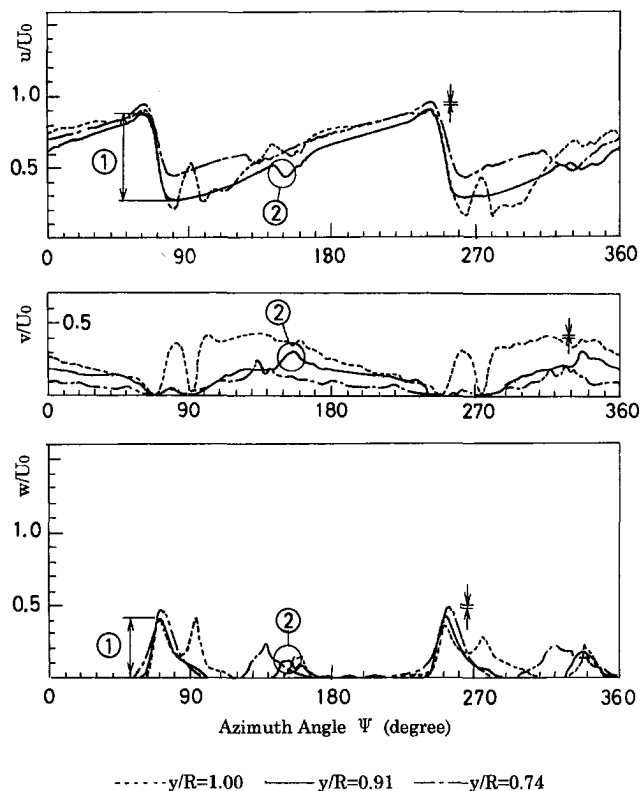


Fig. 7(b) Three components (axial, tangential, radial) of velocity distributions downwind of the model wind turbine rotor with a Mie type tip vane ($x/R = 0.12$); (uncertainty in $u/U_0 = 0.9 \pm 0.004$, $v/U_0 = 0.4 \pm 0.002$, $w/U_0 = 0.5 \pm 0.002$ and $\Psi = 360 \pm 1$)

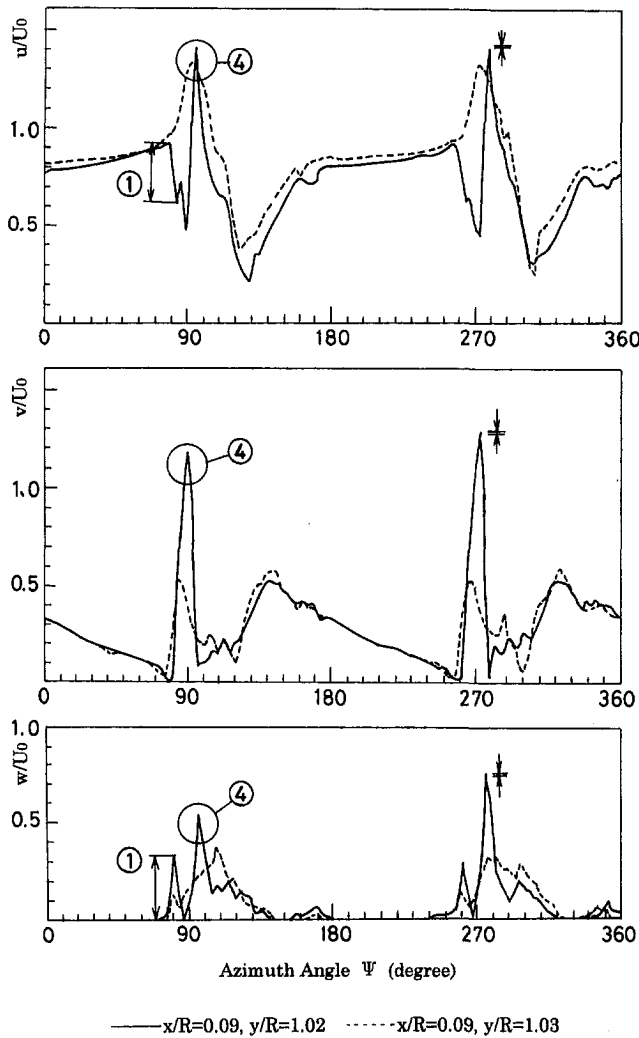


Fig. 8 Three components (axial, tangential, and radial) of velocity distributions just downwind of the Mie type tip vane (uncertainty in $u/U_0 = 1.4 \pm 0.006$, $v/U_0 = 1.3 \pm 0.006$, $w/U_0 = 0.8 \pm 0.004$ and $\Psi = 360 \pm 1$)

rapidly outside $y/R = 1.0$ than that for the blade without the Mie vane. The fluctuation Δu for the blade with a vane takes larger values than those without a vane.

Figure 10 shows the distribution of the amplitude of the tangential velocity, Δw , against the spanwise position. The amplitude Δw indicates a similar tendency as the axial component

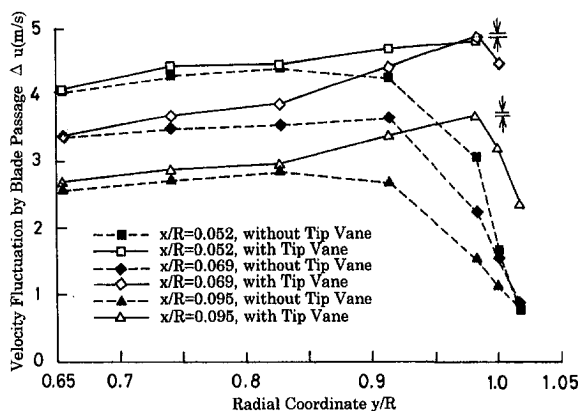


Fig. 9 Spanwise distribution of velocity amplitude Δu due to a blade passage (uncertainty in $\Delta u = 5 \pm 0.02$ and $y/R = 1.0 \pm 0.005$)

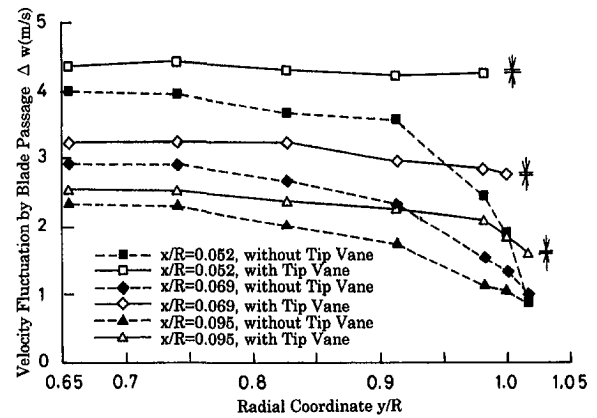


Fig. 10 Spanwise distribution of tangential velocity amplitude Δw due to a blade passage (uncertainty in $\Delta w = 4.2 \pm 0.02$ and $y/R = 1.0 \pm 0.005$)

Δu . The magnitude of Δw without a Mie vane decreases near the blade tip similar to Δu depicted in Fig. 9. It can be seen very clearly that, in the case of application of the Mie vane, the amplitude Δw remains almost constant in the region of $0 < x/R < 0.073$.

Circulation. The velocity \bar{u} induced by a vortex is proportional to the circulation strength Γ and it is inversely proportional to the distance r from the rotor plane. If the vortex filament is assumed to be infinitely long, that is, two-dimensional, the induced velocity is given according to the Biot-Savart's laws by

$$\bar{u} = \frac{\Gamma}{2\pi r} \quad (1)$$

It can be shown after Vermeer and Bussel (1989), that for both Δu and Δw the following relation holds:

$$\Delta u, \Delta w = \frac{\Gamma}{2\pi x} \quad (2)$$

The circulation strength can then be obtained by the detailed measurements of both the axial distance and the induced velocity. Equation (2) can be transformed into

$$\Gamma = 2\pi \left(\frac{\partial(1/\Delta u)}{\partial x} \right)^{-1} \quad (3)$$

and is also valid for Δw . The use of Eq. (3) has the advantage

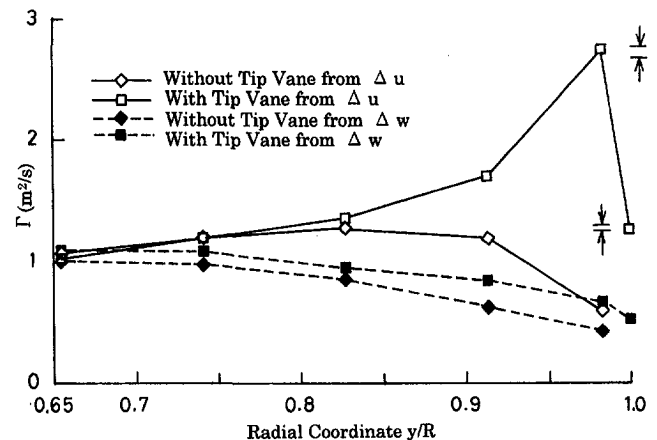


Fig. 11 Spanwise distribution of circulation strength Γ (uncertainty in $\Gamma = 2.8 \pm 0.04$ and $y/R = 1.0 \pm 0.005$)

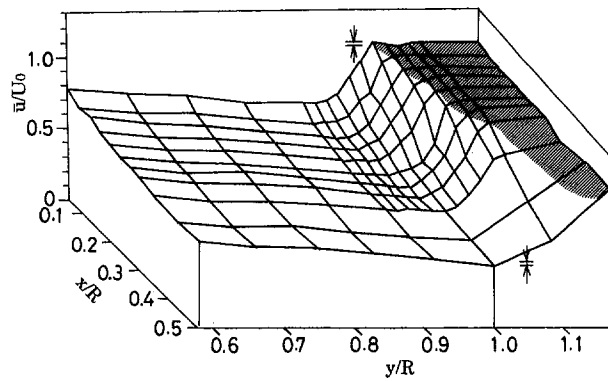


Fig. 12 Distribution of axial time-averaged velocity without a Mie type tip vane (uncertainty in $\bar{u}/U_0 = 0.8 \pm 0.004$ and $x/R = 0.5 \pm 0.005$ and $y/R = 1.0 \pm 0.005$)

that it is independent of the exact distance x between the probe and the bound vorticity at the rotor blade. This procedure has first been used by Vermeer and Bussel (1989). The circulation is estimated with Eq. (3) using the measured velocity determined by the hot wire anemometer. One should be aware that the measured velocity includes the effects of the tip vortex and the existence of the vane. Figure 11 shows the distribution of the circulation strength Γ along the spanwise position as calculated from Δu (■ and □) and from Δw (◆ and ◇). The uncertainty of Γ is almost the three times of the error of Δu , because the terms of Δv and Δw are omitted in calculating Γ .

In the case of taking the Mie vane off, the circulation strength Γ based on Δu is decreasing towards the blade tip. The value of the calculated circulation, however, does not completely vanish at the blade tip. This is caused by the assumption that the vortex filament is infinitely long. For the situation with the Mie vane, the circulation inside the blade shows a similar tendency. However, it gradually increases towards the blade tip, showing a maximum value near the blade tip, and then a sharp decrease in the proximity of the blade tip. It must be realized that the position and strength of the vortex filaments around the Mie vane near the blade tip have an effect on the inflow at the blade.

The real circulation strength Γ can not be determined so far since the procedure used here assumes a two-dimensional vorticity. By measurements in the wake downwind of the turbine as depicted in Figs. 12-15 and the visualization shown by Shimizu et al. (1994b), it can be concluded that the vorticity is largely transformed from the blade tip to the Mie vane.

The circulation estimated by the velocity amplitude Δw decreases towards the blade tip both for the blade with a Mie vane and without a Mie vane. The circulation with the Mie vane takes quantitatively larger value than those without the vane.

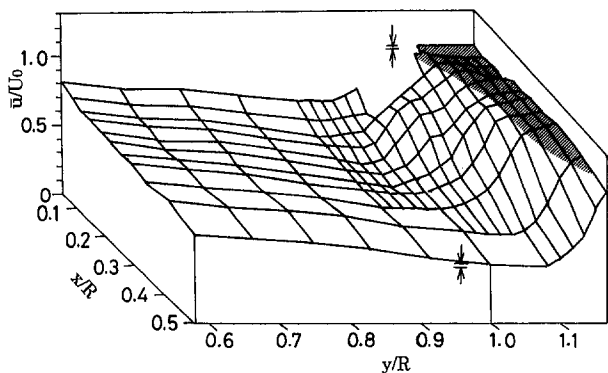


Fig. 13 Distribution of axial time-averaged velocity with a Mie type tip vane (uncertainty in $\bar{u}/U_0 = 0.8 \pm 0.004$ and $x/R = 0.5 \pm 0.005$ and $y/R = 1.0 \pm 0.005$)

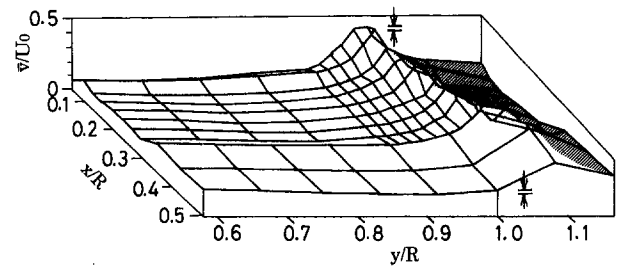


Fig. 14 Distribution of radial time-averaged velocity without a Mie type tip vane (uncertainty in $\bar{v}/U_0 = 0.4 \pm 0.002$ and $x/R = 0.5 \pm 0.005$ and $y/R = 1.0 \pm 0.005$)

Velocity Distribution of Wake. Figures 12 and 13 show the distribution of the time-averaged axial velocity \bar{u} measured at several downwind position with respect to the wind turbine. Figure 12 shows the results for the rotor without the Mie vane. Non-dimensional wind velocity \bar{u}/U_0 outside the blade tip takes nearly the value 1.0, where the velocity inside the blade tip is reduced to about 70 percent on the average. The boundary between the wake and the uniform stream is extended radially outward, as the measurement position is moved downwind. For the rotor with the Mie vane, the velocity reduction has almost the same value as that without the Mie vane as shown in Fig. 13. In the case of application of the Mie vane, the region of the wake, however, is more extended radially outward than that without vane. The velocity of the wake increases gradually in the radial direction. The region of the wake extends largely in terms of the time-averaged value of the unsteady axial velocity.

Figures 14 and 15 show the distribution of the time-averaged radial velocity \bar{v} . The radial velocity \bar{v} takes the maximum value along the boundary between the wake and the uniform stream. The maximum velocity under the condition with the Mie vane is much smaller than that without the Mie vane. It is known that the radial component of the velocity is closely related with the tip vortex. Considering this and the results by Shimizu et al. (1994b), it can be concluded that the vortex generated from the downstream edge of the Mie vane is smaller than the tip vortex of the rotor without the Mie vane. There is a gradual leveling off of the bound vorticity over the downstream side of the vane.

Conclusions

Through the investigations discussed in this paper, the following findings have become evident:

- (1) The Mie vane has a suppressive effect on the formation of the tip vortex on the blade. The released position of the tip vortex is moved to the downstream edge of the Mie vane. The strength of the tip vortex is smaller for the blade with the Mie vane than for the blade without it.

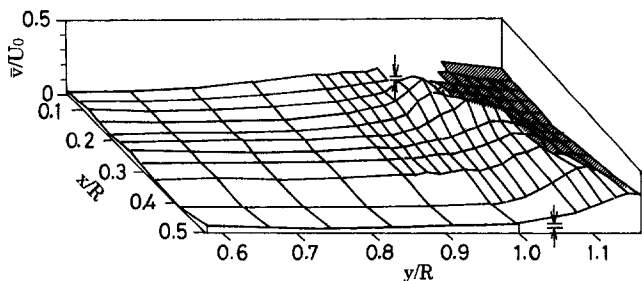


Fig. 15 Distribution of radial time-averaged velocity with a Mie type tip vane (uncertainty in $\bar{v}/U_0 = 0.2 \pm 0.001$ and $x/R = 0.5 \pm 0.005$ and $y/R = 1.0 \pm 0.005$)

(2) It is seen that the circulation persists up to the blade tip due to the presence of the Mie vane.

(3) The Mie vane extends the diameter of the wake downwind of the wind turbine.

Acknowledgment

The authors would like to thank Mr. Nord-Jan. Vermeer, Delft University of Technology, for his advice and for sharing his outstanding knowledge about the interpretation of velocity measurements in the wake of wind turbine model rotors.

References

- Gyatt, G. W., and Lissaman, P. B. S., 1985, "Development and Testing of Tip Devices for Horizontal Axis Wind Turbines," Aero Vironment Inc., DOE/NASA/0341-1, NASA CR-174991, AV-FR-85/802.
- Shimizu, Y., et al., 1990, "Power Augmentation Effects of Horizontal Axis Wind Turbine by Tip Vane (1st Report, Relationships between turbine performance and configuration of tip vanes)," *Trans. JSME*, Vol. B-522, pp. 495-501 (in Japanese).
- Shimizu, Y., et al., 1991, "Power Augmentation of Horizontal Axis Wind Turbine with Tip Vane," *Trans. JSME*, Vol. B-543, pp. 3845-3850 (in Japanese).
- Shimizu, Y., et al., 1994a, "Power Augmentation Effects of a Horizontal Axis Wind Turbine With a Tip Vane-Part 1: Turbine Performance and Tip Vane Configuration," *ASME Journal of Fluids Engineering*, Vol. 116, pp. 287-292.
- Shimizu, Y., et al., 1994b, "Power Augmentation Effects of a Horizontal Axis Wind Turbine With a Tip Vane-Part 2: Flow Visualization," *ASME Journal of Fluids Engineering*, Vol. 116, pp. 293-297.
- Shimizu, Y., et al., 1994c, "Rotation Speed Control of Horizontal Axis Wind Turbine by Tip Vane," *JSME International Journal*, Ser. B, Vol. 37, No. 2, pp. 363-368.
- Tutui, Y., et al., 1988, "LDV Measurements of a Flow Field around a Wind Turbine," *Trans. JSME*, Vol. B-505, pp. 2471-2477 (in Japanese).
- Van Bussel, G. J. W., 1986, "Status Rep. Tipvane Res," EWEA Conference, Rome, pp. 691-695.
- Van Bussel, G. J. W., 1990, "A momentum theory for winglets on horizontal axis wind turbine rotor and some comparison with experiments," *Proceedings of 4th IEA Symposium on the Aerodynamics of Wind Turbines*, Rome, Italy.
- Van Holten, 1976, "Windmills with Diffuser Effect Induced by Small Tip Vanes," *Proc. Int. Symp. Wind Energy Syst.*, Cambridge, U.K.
- Vermeer, N. J., and Van Bussel, G. J. W., 1989, "Velocity measurements in the near wake of a model rotor and comparison with theoretical results," *Proceedings of 15th European Rotational Forum*, Amsterdam, The Netherlands.